Transcranial Optical Monitoring of Cerebrovascular Hemodynamics in Acute Stroke Patients

Turgut Durduran[†,◇]**, Chao Zhou** [◇]**, Brian L Edlow**[‡]**,
Guoqiang Yu**[◇]**, Regine Choe**[◇]**, Meeri N Kim**[◇]**, Brett L
Cucchiara**[‡]**, Mary E Putt**[+]**, Qaisar Shah**[‡]**, Scott E Kasner**[‡]**,
Joel H Greenberg**[‡]**, Arjun G Yodh**[◇]**, John A Detre**[‡,†]

Departments of: [†]*Radiology,* [◇]*Physics* & *Astronomy,* [+]*Biostatistics* &
Epidemiology, [‡]*Neurology, University of Pennsylvania*
*Corresponding Author: Turgut Durduran, 209 South 33rd Str, Philadelphia, PA
19104, Tel: 1-215-898-5148, Fax: 1-215-573-6391*

durduran@alumni.upenn.edu

http://www.physics.upenn.edu/yodhlab

Abstract: "Diffuse correlation spectroscopy" (DCS) is a technology
for non-invasive transcranial measurement of cerebral blood flow
(CBF) that can be hybridized with "near-infrared spectroscopy"
(NIRS). Taken together these methods hold potential for monitoring
hemodynamics in stroke patients. We explore the utility of DCS
and NIRS to measure effects of head-of-bed (HOB) positioning at
30°, 15°, 0°, -5° and 0° angles in patients with acute ischemic stroke
affecting frontal cortex and in controls. HOB positioning significantly
altered CBF, oxy-hemoglobin (HbO_2) and total-hemoglobin (THC)
concentrations. Moreover, the presence of an ipsilateral infarct was a
significant effect for all parameters. Results are consistent with the
notion of impaired CBF autoregulation in the infarcted hemisphere.

© 2009 Optical Society of America

OCIS codes: (170.3880) Medical and biological imaging; (170.3340) Laser
Doppler velocimetry; (170.5280) Photon migration; (170.6480) Spectroscopy,
speckle; (280.1415) Biological sensing and sensors

References and links

1. A. D. Lopez, C. D. Mathers, M. Ezzati, D. T. Jamison, and C. J. L. Murray, "Global and regional burden of disease and risk factors, 2001: systematic analysis of population health data," The Lancet **367**(9524), 1747–1757 (2006).
2. European Stroke Organization, "Recommendations for Stroke Management," http://www.eso-stroke.org/recommendations.php?cid=9&sid=1 (Last Accessed: January 28, 2009).
3. C. Benesch and R. Holloway, "Economic Impact of Stroke and Implications for Interventions." CNS Drugs **9**, 19 (1998).
4. L. B. Goldstein, "Should antihypertensive therapies be given to patients with acute ischemic stroke?" Drug Saf **22**(1), 13–18 (2000).
5. S. L. Dawson, R. B. Panerai, and J. F. Potter, "Serial changes in static and dynamic cerebral autoregulation after acute ischaemic stroke," Cerebrovasc Dis **16**(1), 69–75 (2003).
6. K. A. Hossmann, "Viability thresholds and the penumbra of focal ischemia," Ann Neurol **36**(4), 557–565 (1994).

7. J. Astrup, B. K. Siesjo, and L. Symon, "Thresholds in cerebral ischemia - the ischemic penumbra," Stroke **12**(6), 723–725 (1981).

8. M. Wintermark, M. Sesay, E. Barbier, K. Borbely, W. P. Dillon, J. D. Eastwood, T. C. Glenn, C. B. Grandin, S. Pedraza, J. F. Soustiel, T. Nariai, G. Zaharchuk, J. M. Caille, V. Dousset, and H. Yonas, "Comparative overview of brain perfusion imaging techniques," Stroke **36**(9), 83–99 (2005).

9. J. C. Baron, "Mapping the ischaemic penumbra with PET: a new approach," Brain **124**(Pt 1), 2–4 (2001).

10. M. H. Mahagne, O. David, J. Darcourt, O. Migneco, A. Dunac, M. Chatel, and J. C. Baron, "Voxel-based mapping of cortical ischemic damage using Tc 99m L,L-ethyl cysteinate dimer SPECT in acute stroke," J Neuroimaging **14**(1), 23–32 (2004).

11. R. E. Latchaw, "Cerebral perfusion imaging in acute stroke," J Vasc Interv Radiol **15**(1 Pt 2), 29–46 (2004).

12. J. A. Chalela, D. C. Alsop, J. B. Gonzalez-Atavales, J. A. Maldjian, S. E. Kasner, and J. A. Detre, "Magnetic resonance perfusion imaging in acute ischemic stroke using continuous arterial spin labeling," Stroke **31**(3), 680–687 (2000).

13. C. C. Bishop, S. Powell, D. Rutt, and N. L. Browse, "Transcranial Doppler measurement of middle cerebral artery blood flow velocity: a validation study," Stroke **17**, 913–915 (1986).

14. R. R. Pindzola, J. R. Balzer, E. M. Nemoto, S. Goldstein, and H. Yonas, "Cerebrovascular reserve in patients with carotid occlusive disease assessed by stable xenon-enhanced ct cerebral blood flow and transcranial Doppler," Stroke **32**(8), 1811–1817 (2001).

15. A. V. Alexandrov, A. M. Demchuk, T. H. Wein, and J. C. Grotta, "Yield of transcranial Doppler in acute cerebral ischemia," Stroke **30**(8), 1604–1609 (1999).

16. S. Schwarz, D. Georgiadis, A. Aschoff, and S. Schwab, "Effects of body position on intracranial pressure and cerebral perfusion in patients with large hemispheric stroke," Stroke **33**(2), 497–501 (2002).

17. A. Villringer and B. Chance, "Non-invasive optical spectroscopy and imaging of human brain function," Trends Neurosci. **20**, 435–442 (1997).

18. E. M. C. Hillman, "Optical brain imaging in vivo: techniques and applications from animal to man," Journal of Biomedical Optics **12**(5) (2007).

19. W. M. Kuebler, "How NIR is the future in blood flow monitoring?" J Appl Physiol **104**(4), 905–906 (2008).

20. R. Carandang and D. W. Krieger, "Near infrared spectroscopy: finding utility in malignant hemispheric stroke," Neurocritical Care **6**(3), 161–164 (2007).

21. C. Terborg, S. Bramer, S. Harscher, M. Simon, and O. W. Witte, "Bedside assessment of cerebral perfusion reductions in patients with acute ischaemic stroke by near-infrared spectroscopy and indocyanine green," J Neurol Neurosurg Psychiatry **75**(1), 38–42 (2004).

22. A. Liebert, H. Wabnitz, J. Steinbrink, M. Moller, R. Macdonald, H. Rinneberg, A. Villringer, and H. Obrig, "Bed-side assessment of cerebral perfusion in stroke patients based on optical monitoring of a dye bolus by time-resolved diffuse reflectance," Neuroimage **24**, 426–35 (2005).

23. E. Keller, G. Wietasch, P. Ringleb, M. Scholz, S. Schwarz, R. Stingele, S. Schwab, D. Hanley, and W. Hacke, "Bedside monitoring of cerebral blood flow in patients with acute hemispheric stroke," Crit Care Med **28**(2), 511–516 (2000).

24. F. Vernieri, N. Rosato, F. Pauri, F. Tibuzzi, F. Passarelli, and P. M. Rossini, "Near Infrared Spectroscopy and Transcranial Doppler in Monohemispheric Stroke," Eur Neurol **41**(3), 159–162 (1999).

25. P. Bönöczk, G. Panczel, and Z. Nagy, "Vinpocetine increases cerebral blood flow and oxygenation in stroke patients: a near infrared spectroscopy and transcranial Doppler study," European Journal of Ultrasound **15**(1-2), 85–91 (2002).

26. K. Sakatani, Y. Xie, W. Lichty, S. Li, and H. Zuo, "Language-Activated Cerebral Blood Oxygenation and Hemodynamic Changes of the Left Prefrontal Cortex in Poststroke Aphasic Patients : A Near-Infrared Spectroscopy Study," Stroke **29**(7), 1299–1304 (1998).

27. H. Kato, M. Izumiyama, H. Koizumi, A. Takahashi, and Y. Itoyama, "Near-Infrared Spectroscopic Topography as a Tool to Monitor Motor Reorganization After Hemiparetic Stroke: A Comparison With Functional MRI," Stroke **33**(8), 2032–2036 (2002).

28. I. Miyai, H. Yagura, M. Hatakenaka, I. Oda, I. Konishi, and K. Kubota, "Longitudinal Optical Imaging Study for Locomotor Recovery After Stroke," Stroke **34**(12), 2866–2870 (2003).

29. M. S. Damian and R. Schlosser, "Bilateral near infrared spectroscopy in space-occupying middle cerebral artery stroke," Neurocritical Care **6**(3), 165–173 (2007).

30. D. Hargroves, R. Tallis, V. Pomeroy, and A. Bhalla, "The influence of positioning upon cerebral oxygenation after acute stroke: a pilot study," Age Ageing **37**(5), 581–585 (2008).

31. D. A. Boas, L. E. Campbell, and A. G. Yodh, "Scattering and Imaging with Diffusing Temporal

Field Correlations," Phys Rev Lett **75**(9), 1855–1858 (1995).

32. D. A. Boas and A. G. Yodh, "Spatially varying dynamical properties of turbid media probed with diffusing temporal light correlation," J. Opt. Soc. Am. A **14**(1), 192–215 (1997).

33. D. J. Pine, D. A. Weitz, P. M. Chaikin, and Herbolzheimer, "Diffusing-wave spectroscopy," Phys. Rev. Lett. **60**, 1134–1137 (1988).

34. G. Maret and P. E. Wolf, "Multiple light scattering from disordered media. The effect of brownian motion of scatterers," Z. Phys. B **65**, 409–413 (1987).

35. T. Durduran, "Non-Invasive Measurements of Tissue Hemodynamics with Hybrid Diffuse Optical Methods," Ph.D. Dissertation, University of Pennsylvania (2004).

36. T. Durduran, G. Yu, M. G. Burnett, J. A. Detre, J. H. Greenberg, J. Wang, C. Zhou, and A. G. Yodh, "Diffuse Optical Measurements of Blood Flow, Blood Oxygenation and Metabolism in Human Brain during Sensorimotor Cortex Activation," Opt Lett **29**, 1766–1768 (2004).

37. J. Li, G. Dietsche, D. Iftime, S. E. Skipetrov, G. Maret, T. Elbert, B. Rockstroh, and T. Gisler, "Noninvasive detection of functional brain activity with near-infrared diffusing-wave spectroscopy," J Biomed Opt **10**(4), 044,002–1–044,002–12 (2005).

38. G. Yu, T. Durduran, C. Zhou, H. W. Wang, M. E. Putt, M. Saunders, C. M. Seghal, E. Glatstein, A. G. Yodh, and T. M. Busch, "Noninvasive Monitoring of Murine Tumor Blood Flow During and After Photodynamic Therapy Provides Early Assessment of Therapeutic Efficacy," Clin. Cancer Res. **11**, 3543–3552 (2005).

39. E. M. Buckley, M. N. Kim, T. Durduran, G. Yu, R. Choe, C. Zhou, S. Shultz, C. M. Sehgal, D. J. Licht, P. H. Arger, H. H. Hurt, N. M. Cook, and A. G. Yodh, "Monitoring Hemodynamic Changes in Preterm Infants Using Optical Spectroscopies and Doppler Ultrasound," in *OSA Biomedicals Topicals*, p. CN279 (St Petersburg, FL, 2008).

40. C. Menon, G. M. Polin, I. Prabakaran, A. Hs, C. Cheung, J. P. Culver, J. . Pingpank, C. S. Sehgal, A. G. Yodh, D. G. Buerk, and D. L. Fraker, "An Integrated Approach to Measuring Tumor Oxygen Status using Human Melanoma Xenografts as a Model," Cancer Res. **63**, 7232–40 (2003).

41. T. Durduran, M. N. Kim, E. M. Buckley, R. Choe, C. Zhou, G. Y. Yu, and A. G. Yodh, "Validation of diffuse correlation spectroscopy for measurement of cerebral blood flow across spatial scales and against multiple modalities," in *SPIE Photonics West* (San Jose, CA, 2009).

42. T. Durduran, C. Zhou, M. N. Kim, E. M. Buckley, G. Yu, R. Choe, S. M. Durning, S. Mason, L. M. Montenegro, S. C. Nicholson, R. A. Zimmerman, J. J. Wang, J. A. Detre, A. G. Yodh, and D. J. Licht, "Validation of Diffuse Correlation Spectroscopy for Non-Invasive, Continuous Monitoring of CBF in Neonates with Congenital Heart Defects," in *Annual Meeting of the American Neurological Association*, p. Abstract 299 (American Neurological Association, Salt Lake City, Utah, 2008).

43. T. Durduran, C. Zhou, G. Yu, R. Choe, D. Silvestre, J. J. Wang, S. Nicolson, L. Montenegro, J. A. Detre, A. G. Yodh, and D. Licht, "Preoperative measurement of CO2 reactivity and cerebral autoregulation in neonates with severe congenital heart defects," in *SPIE Photonics West* (San Jose, CA, 2007).

44. G. Yu, T. Floyd, T. Durduran, C. Zhou, J. J. Wang, J. A. Detre, and A. G. Yodh, "Validation of diffuse correlation spectroscopy for muscle blood flow with concurrent arterial-spin-labeling perfusion," Opt Exp **15**, 1064–75 (2007).

45. M. N. Kim, T. Durduran, S. Frangos, E. M. Buckley, C. Zhou, G. Yu, H. Moss, B. L. Edlow, E. Maloney-Wilensky, J. A. Detre, J. H. Greenberg, W. A. Kofke, A. G. Yodh, M. S. Grady, J. H. Woo, R. L. Wolf, and J. Levine, "Validation Of Diffuse Correlation Spectroscopy Against Xenon CTCBF In Humans After Traumatic Brain Injury or Subarachnoid Hemorrhage," in *Neurocritical Care Society Annual Meeting* (Miami, FL, 2008).

46. T. Durduran, M. N. Kim, E. M. Buckley, C. Zhou, G. Yu, R. Choe, J. H. Greenberg, J. A. Detre, and A. G. Yodh, "Diffuse Optical Monitoring of Cerebral Oxygen Metabolism at the Bed-Side in Cerebrovascular Disorders," in *OSA: Annual Meeting, Frontiers in Optics 2008* (Rochester, NY, 2008).

47. C. Zhou, S. Eucker, T. Durduran, G. Yu, J. Ralston, S. Friess, R. Ichor, S. Margulies, and A. G. Yodh, "Diffuse Optical Monitoring of Hemodynamic Changes in Piglet Brain with Closed Head Injury," Journal of Neurotrauma **submitted** (2009).

48. J. P. Culver, T. Durduran, D. Furuya, C. Cheung, J. H. Greenberg, and A. G. Yodh, "Diffuse Optical Tomography of Cerebral Blood Flow, Oxygenation and Metabolism in Rat During Focal Ischemia," J. Cereb. Blood Flow Metab. **23**, 911–24 (2003).

49. C. Cheung, J. P. Culver, K. Takahashi, J. H. Greenberg, and A. G. Yodh, "In vivo cerebrovascular measurement combining diffuse near-infrared absorption and correlation spectroscopies," Phys. Med. and Biol. **46**(8), 2053–2065 (2001).

50. C. Zhou, G. Yu, D. Furuya, J. H. Greenberg, A. G. Yodh, and T. Durduran, "Diffuse Optical Correlation tomography of cerebral blood flow during cortical spreading depression in rat brain,"

Opt. Exp **14**, 1125–44 (2006).

51. T. Durduran, M. N. Kim, E. M. Buckley, B. L. Edlow, H. Moss, C. Zhou, G. Yu, R. Choe, S. K. Frangos, E. Wilensky-Mahoney, A. Kofke, J. M. Levine, R. L. Wolf, J. Woo, S. E. Kasner, B. L. Cucchiara, M. E. Putt, A. G. Yodh, J. H. Greenberg, and J. A. Detre, "Bedside Monitoring of Cerebral Hemodynamics for Stroke and Neurocritical Care Using Novel Diffuse Optical Probes," in *Annual Meeting of the American Neurological Association*, p. Abstract 298 (American Neurological Association, Salt Lake City, Utah, 2008).

52. T. Durduran, C. Zhou, B. L. Edlow, G. Yu, R. Choe, B. L. Cucchiara, M. Putt, Q. Shah, S. E. Kasner, A. G. Yodh, J. H. Greenberg, and J. A. Detre, "CBF During Changes in Head of Bed Position in Acute, Ischemic Stroke Monitored at the bed-side: hemispheric effect of infarct," in *BRAIN 07, International Society of Cerebral Blood Flow and Metabolism* (Osaka, Japan, 2007).

53. T. Durduran, C. Zhou, G. Yu, B. Edlow, R. Choe, Q. Shah, S. E. Kasner, B. L. Cucchiara, A. G. Yodh, J. H. Greenberg, and J. A. Detre, "Bed-side Monitoring of Cerebral Blood Flow (CBF) in Acute Stroke Patients During Changes in Head of Bed Position," in *International Stroke Conference*, vol. P37 (American Heart Association, 2007).

54. M. N. Kim, T. Durduran, S. Frangos, E. M. Buckley, C. Zhou, G. Yu, B. L. Edlow, E. Mahoney-Wilensky, S. M. Grady, J. Levine, J. A. Detre, J. H. Greenberg, and A. G. Yodh, "Diffuse Optical Measurements of Cerebral Blood Flow and Oxygenation in Patients after Traumatic Brain Injury or Subarachnoid Hemhorrage," in *OSA Biomedicals Topicals*, p. CN237 (St Petersburg, FL, 2008).

55. G. Yu, T. Durduran, G. Lech, C. Zhou, B. Chance, E. R. Mohler, and A. G. Yodh, "Time-dependent Blood Flow and Oxygenation in Human Skeletal Muscle Measured with Noninvasive Near-infrared Diffuse Optical Spectroscopies," J Biomed Opt **10**(3), 024,027–1–12 (2005).

56. G. Yu, T. Durduran, C. Zhou, T. C. Zhu, J. C. Finlay, T. M. Busch, S. B. Malkowicz, S. M. Hahn, and A. G. Yodh, "Real-time In situ Monitoring of Human Prostate Photodynamic Therapy with Diffuse Light," Photochem Photobiol **82**, 1279–84 (2006).

57. U. Sunar, H. Quon, T. Durduran, J. Zhang, J. Du, C. Zhou, G. Yu, R. Choe, A. Kilger, R. Lustig, L. Loevner, S. Nioka, B. Chance, and A. G. Yodh, "Non-invasive diffuse optical measurement of blood flow and blood oxygenation for monitoring radiation therapy in patients with head and neck tumors: a pilot study," J Biomed Opt **11**, 064,021 (2006).

58. C. Zhou, R. Choe, N. Shah, T. Durduran, G. Yu, A. Durkin, D. Hsiang, R. Mehta, J. Butler, A. Cerussi, B. J. Tromberg, and A. G. Yodh, "Diffuse optical monitoring of blood flow and oxygenation in human breast cancer during early stages of neoadjuvant chemotherapy," J Biomed Opt **12**(5), 051,903 (2007).

59. U. Sunar, S. Makonnen, C. Zhou, T. Durduran, G. Yu, H. W. Wang, W. M. Lee, and A. G. Yodh, "Hemodynamic responses to antivascular therapy and ionizing radiation assessed by diffuse optical spectroscopies," Opt. Express **15**(23), 15,507–15,516 (2007).

60. T. Durduran, R. Choe, G. Yu, C. Zhou, J. C. Tchou, B. J. Czerniecki, and A. G. Yodh, "Diffuse Optical Measurement of Blood flow in Breast Tumors," Opt Lett **30**, 2915–17 (2005).

61. H. P. Adams, B. H. Bendixen, L. J. Kappelle, J. Biller, B. B. Love, D. L. Gordon, and E. E. Marsh, "Classification of subtype of acute ischemic stroke. Definitions for use in a multicenter clinical trial. TOAST. Trial of Org 10172 in Acute Stroke Treatment," Stroke **24**(1), 35–41 (1993).

62. D. T. Delpy, M. Cope, P. van der Zee, S. Arridge, S. Wray, and J. Wyatt, "Estimation of optical pathlength through tissue from direct time of flight measurement," Phys Med Biol **33**, 1433–1442 (1988).

63. M. Cope and D. T. Delpy, "System for long-term measurement of cerebral blood flow and tissue oxygenation on newborn infants by infra-red transillumination." Med Biol Eng Comput **26**, 289–294 (1988).

64. P. van der Zee, M. Cope, S. R. Arridge, M. Essenpreis, L. A. Potter, A. D. Edwards, J. S. Wyatt, D. C. McCormick, S. C. Toth, E. O. R. Reynolds, and D. T. Delpy, "Experimentally measured optical pathlengths for the adult's head, calf and forearm and the head of the newborn infant asa function of interoptode spacing," Adv. Exp. Med. Biol. **316**, 143–153 (1992).

65. A. Duncan, J. H. Meek, M. Clemence, C. E. Elwell, L. Tyszczuk, M. Cope, and D. T. Delpy, "Optical pathlength measurements on adult head, calf and forearm and the head of the newborn infant using phase resolved optical spectroscopy," Phys. Med. Biol. **40**(2), 295–304. (1995).

66. M. Kohl, C. Nolte, H. R. Heekeren, S. Horst, U. Scholz, H. Obrig, and A. Villringer, "Determination of the wavelength dependence of the differential pathlength factor from near-infrared pulse signals," Phys Med Biol **43**(6), 1771–82 (1998).

67. S. R. Arridge, M. Cope, and D. T. Delpy, "The theoretical basis for the determination of optical pathlengths in tissue: temporal and frequency analysis," Phys Med Biol **37**(7), 1531–60 (1992).

68. Compiled by Scott Prahl, Online: http://omlc.ogi.edu/spectra/hemoglobin/summary.html.

69. G. Strangman, M. A. Franceschini, and D. A. Boas, "Factors affecting the accuracy of near-infrared spectroscopy concentration calculations for focal changes in oxygenation parameters,"

NeuroImage **18**, 865–79 (2003).

70. D. A. Boas, T. Gaudette, G. Strangman, X. Cheng, J. J. A. Marota, and J. B. Mandeville, "The Accuracy of Near Infrared Spectroscopy and Imaging during Focal Changes in Cerebral Hemodynamics," NeuroImage **13**, 76–90 (2001).

71. E. Okada and D. T. Delpy, "Near-Infrared light propagation in an adult head model. II. Effect of superficial tissue thickness on the sensitivity of the near-infrared spectroscopy signal," Appl. Opt. **42**, 2915–21 (2003).

72. J. Steinbrink, H. Wabnitz, H. Obrig, A. Villringer, and H. Rinneberg, "Determining changes in NIR absorption using a layered model of the human head," Phys Med Biol **46**(3), 879–96. (2001).

73. A. Einstein, "On the motion of small particles suspended in liquids at rest required by the molecular-kinetic theory of heat," Annalen der Physik **17**, 549–60 (1905).

74. J. C. Pinheiro and D. M. Bates, *Mixed-effects models in S and S-Plus* (Springer, New York, 2000).

75. H. Akaike, "A new look at the statistical model identification," Automatic Control, IEEE Transactions on **19**(6), 716–723 (1974).

76. A. Chieregato, A. Tanfani, C. Compagnone, R. Pascarella, L. Targa, and E. Fainardi, "Cerebral blood flow in traumatic contusions is predominantly reduced after an induced acute elevation of cerebral perfusion pressure," Neurosurgery **60**(1), 115–123 (2007).

77. P. Langhorne, D. J. Stott, L. Robertson, J. MacDonald, L. Jones, C. McAlpine, F. Dick, G. S. Taylor, and G. Murray, "Medical complications after stroke: a multicenter study," Stroke **31**(6), 1223–1229 (2000).

78. R. Fernandez-Crehuet, C. Diaz-Molina, J. de Irala, D. Martinez-Concha, I. Salcedo-Leal, and J. Masa-Calles, "Nosocomial infection in an intensive-care unit: identification of risk factors." Infect Control Hosp Epidemiol **18**(12), 825–30 (1997).

79. S. I. Kamran, D. Downey, and R. L. Ruff, "Pneumatic sequential compression reduces the risk of deep vein thrombosis in stroke patients," Neurology **50**(6), 1683–1688 (1998).

80. J. Kelly, A. Rudd, R. Lewis, and B. J. Hunt, "Venous thromboembolism after acute stroke," Stroke **32**(1), 262–267 (2001).

81. C. Dohmen, B. Bosche, R. Graf, T. Reithmeier, R. I. Ernestus, G. Brinker, J. Sobesky, and W. D. Heiss, "Identification and clinical impact of impaired cerebrovascular autoregulation in patients with malignant middle cerebral artery infarction," Stroke **38**(1), 56–61 (2007).

82. A. W. Wojner-Alexander, Z. Garami, O. Y. Chernyshev, and A. V. Alexandrov, "Heads down: flat positioning improves blood flow velocity in acute ischemic stroke," Neurology **64**(8), 1354–1357 (2005).

83. W. K. Paula, "Heads down: flat positioning improves blood flow velocity in acute ischemic stroke," Neurology **65**(9), 1514–1514 (2005).

84. L. A. Lipsitz, S. Mukai, J. Hamner, M. Gagnon, and V. Babikian, "Dynamic regulation of middle cerebral artery blood flow velocity in aging and hypertension," Stroke **31**(8), 1897–1903 (2000).

85. T. Asil, U. Utku, K. Balci, and I. Uzunca, "Changing cerebral blood flow velocity by transcranial Doppler during head up tilt in patients with diabetes mellitus," Clin Neurol Neurosurg **109**(1), 1–6 (2007).

86. J. Adams, Harold P, G. del Zoppo, M. J. Alberts, D. L. Bhatt, L. Brass, A. Furlan, R. L. Grubb, R. T. Higashida, E. C. Jauch, C. Kidwell, P. D. Lyden, L. B. Morgenstern, A. I. Qureshi, R. H. Rosenwasser, P. A. Scott, and E. F. Wijdicks, "Guidelines for the Early Management of Adults With Ischemic Stroke," .

1. Introduction

Ischemic stroke is the leading cause of morbidity and long term disability in Europe and the United States and is among the leading causes of death [1, 2]. It is also the second leading cause of dementia (after Alzheimer's disease). The projected cost of stroke care will reach trillions of dollars over the next five decades. Stroke accounts for nearly 10% of deaths in the Western hemisphere and about 5% of health-care costs [3]. Thus, although some progress has been made in the primary and secondary prevention of stroke and in its acute management, there remains a pressing need for additional strategies to reduce the burden of stroke on individual patients and on society.

The goal of most medical interventions in acute ischemic stroke care is to maximize blood perfusion in the affected region and surrounding ischemic penumbra by increasing local and/or global cerebral blood flow (CBF). Intervention strategies to increase CBF are based on the premise that normal autoregulation of CBF is disrupted and

perfusion of the infarcted and penumbral regions are dependent on perfusion pressure [4, 5]. These interventions include keeping the patient flat, intravenous hydration, withholding anti-hypertensive therapy, and hypertensive therapy with pressor drugs. In practice, however, brain perfusion is rarely measured and a measurement of local microvascular CBF is almost entirely inaccessible. Furthermore, neurological symptoms may not occur until CBF drops to 40% of normal, and prolonged periods of cerebral ischemia increase the likelihood that neurological symptoms will become irreversible as CBF further drops to 20% of normal [6, 7]. The ability to measure CBF at the bedside would provide new opportunities for study of cerebrovascular autoregulation, permitting hemodynamic interventions to be optimized, and potentially administered before the onset of neurological symptoms. Furthermore, because of the high prevalence of stroke and the enormous cost of its management, even strategies with modest benefits are worth pursuing.

To date, imaging modalities such as oxygen-15 positron emission tomography (^{15}O-PET), single-photon emission computed tomography (SPECT), dynamic susceptibility contrast or arterial spin labeled bolus tracking perfusion MRI (ASL-MRI), and Xenon enhanced computed tomography (Xenon-CT) have been used to measure CBF in stroke patients [8–12]. However, because they are costly and are not portable, these methods tend to be used once, if at all, during the course of a patient's hospitalization. Furthermore, CBF can only be measured while the patient is supine for MRI, PET and CT techniques.

The primary clinical modality for serial monitoring of CBF at the bedside is the Transcranial Doppler (TCD) ultrasonography [13] technique which measures flow velocities in the major arteries. However, only the proximal portions of the intracranial arteries can be insonated and TCD provides no information about microvasculature perfusion through collateral vessels. Furthermore, since velocity changes predict CBF variation only if vessel diameters do not change, TCD has limited utility in stroke evaluation [14], with the best success in patients with proximal arterial occlusions [15]. Nevertheless, TCD has been used to monitor the effects of head-of-bed (HOB) positioning on middle cerebral artery (MCA) velocity in patients with large hemispheric strokes [16], finding a decrease with elevation of HOB, but only patients with partial recanalization of the MCA could be studied.

The present study explores the potential of diffuse optics for CBF monitoring at the bedside. Previously, spectroscopic optical monitoring ("near-infrared spectroscopy" (NIRS)) has been used for transcranial measurements of total hemoglobin concentration (THC), blood oxygen saturation [17, 18], and, indirectly, for CBF monitoring using an exogenous tracer [19]. In stroke patients, NIRS studies [20] have explored detection of hemispheric CBF and oxygenation reduction [19, 21–23], cerebrovascular reactivity [24, 25], and local functional changes [26–28]. Some studies have shown utility for monitoring acute ischemic stroke longitudinally [29], providing information complementary to the macrovascular CBF obtained with TCD [24]. Hargroves *et al* [30] have shown that NIRS is able to detect changes in blood oxygen saturation during postural alterations in stroke patients.

"Diffuse correlation spectroscopy" (DCS) (or "diffusing wave spectroscopy" (DWS)) [31–34] is a novel technique that has been applied to characterize blood flow in deep tissues. DCS uses the temporal intensity fluctuations of scattered light to probe CBF. It shares the light penetration advantages of NIRS but provides a much more direct measure of CBF [35–37]. The technique has been extensively validated *in vivo*, in tissues, including comparisons with laser Doppler flowmetry (LDF) [35] , Doppler ultrasound

(DU) [35, 38–40], arterial-spin labeled MRI (ASL-MRI) [35, 36, 41–44], Xenon-CT [45], fluorescent microsphere measurement of CBF [46, 47], and against expectations from invasive and non-invasive measures of physiology [35–37, 48–50]. Recently, its clinical feasibility as a bed-side monitor was also tested for assessing cerebral autoregulation in acute stroke [51–53], in traumatic brain injury [45, 51, 54] and in measuring the carbon dioxide reactivity of neonates with congenital heart defects [42, 43]. In other clinical problems, the feasibility of DCS has been demonstrated for monitoring diseased and healthy human muscle [44, 55], for monitoring prostate, lung, breast and head & neck cancers of humans [56–58] and cancer models in animals [38, 40, 59, 60]. These developments indicate the potential of all-optical methods for continuous non-invasive estimation of cerebral metabolic rate of oxygen extraction (CMRO$_2$) [35, 36, 48–50]. In total, these studies have shown that DCS can reliably provide a flow index proportional to relative changes in CBF.

Here we demonstrate the clinical potential of concurrent bedside optical CBF and THC monitoring in acute ischemic stroke patients. We hypothesized that optical probes placed on the forehead of patients with acute ischemic stroke (AIS) affecting the anterior circulation, would detect differences in autoregulatory impairment between the affected and unaffected hemispheres during head-of-bed (HOB) manipulations. The term autoregulation is used in this manuscript to describe cerebral blood flow changes with HOB positioning. We also compared findings of CBF with concurrent measurements of THC using NIRS.

Seventeen patients with AIS were recruited and studied on one or more occasions during their hospitalization. A comparison group of eight subjects with vascular risk factors was also studied on one occasion. At each time point, changes in CBF (rCBF) and THC (ΔTHC) from each hemisphere were measured sequentially at four HOB positions (30°, 15°, 0°, -5°, and 0°) and normalized to the value at HOB=30° (rCBF$_{30°}$) for comparison between subjects and hemispheres. Throughout this manuscript, "r" denotes "relative" change (i.e. as opposed to "regional" which is sometimes employed in the literature).

Overall, this study demonstrates use of DCS on stroke patients, demonstrates DCS as a new diagnostic tool with the potential to develop into a non-invasive bed-side monitor of local microvascular CBF, and demonstrates the potential of complementary hemodynamic information available by hybridizing NIRS with DCS. DCS-NIRS probes are demonstrated to detect hemispheric differences in cerebrovascular hemodynamics using the simple bedside intervention of altering a patient's head-of-bed (HOB) position. The ability to measure cerebrovascular hemodynamics at the bedside provides new opportunities for individualized stroke care based on each patient's hemodynamics responses to these types of interventions. (Note, part of this data was previously published in abstract form [51–53]).

2. Materials and Methods

2.1. Study Design and Patient Enrollment

This study was conducted at the Hospital of the University of Pennsylvania with a study protocol approved by the local institutional review board. Written consent was provided by subjects or their family members. Two groups of subjects were enrolled: (1) Subjects without stroke but with vascular risk factors (VRF) and age-matched to the stroke group, and (2) patients with acute ischemic stroke (AIS). Race was recorded as Caucasian (C), African American (AA), Asian (A) and other (O) .

Subjects in the VRF group had no neurological deficits and were screened for history

of at least one of the following cardiovascular disease risk factors: hypertension (HTN), diabetes mellitus (DM), hyperlipidemia (LIP), coronary artery disease (CAD), previous myocardial infarction (MYCI), previous stroke (STR), previous transient ischemic attack (TIA), previous or current smoking (TOB) or atrial fibrillation (AFIB). All subjects were using medication for at least one of these conditions. This group was selected to rule out effects due to the advanced age of the AIS group and the common occurence of these risk factors.

The AIS group consisted of patients admitted to the stroke service with radiographic evidence or clinical suspicion of acute ischemic stroke involving the frontal lobe cortex. Exclusion criteria included intracranial hemorrhage on initial CT or MRI scan and inability to lie supine for 15 minutes. Admission NIH Stroke Scale (NIHSS) was scored for each patient at the time of admission. Vascular risk factors identical to those in the VRF group were ascertained from verbal history and available medical records. Stroke etiology was classified according to the "Trial of ORG 10172 in Acute Stroke Treatment" (TOAST) criteria [61] as large-artery atherosclerosis (LAS), small-artery occlusion (SAO), cardioembolic (CE), cryptogenic (CRYP) and other causes (OTHER). A neurologist reviewed all available head CT and brain MRI data to determine stroke (or infarct) laterality ("Stroke Lat."), vascular territory, and region(s) of brain involved. The primary indicators for radiographic evidence of stroke were hypodensity on CT and/or diffusion restriction on diffusion MRI sequences. CT and MR angiographic data were also used to support the assessment of vascular territory involvement where available. Vessel involvement ("Vessel Inv.") was characterized as middle cerebral artery (MCA), anterior cerebral artery (ACA). Brain region involvement ("Brain Reg. Inv.") was characterized as frontal (F), temporal (T), parietal (P) and occipital (O). If orthostasis ("Orth. Symp."), defined by the presence of worsening neurological symptoms with altered HOB position, was observed during the study, it was noted.

Measurements were planned for three separate days. Probes were placed on the forehead about 1.5-2 cm symmetrically left and right of the mid-line in order to avoid sinuses. The probes were held tightly onto the skin with black foam pads using medical tape and a circumferential, black elastic band. Both rCBF and ΔTHC were measured in both frontal lobes for 5 minutes each at HOB angles of 30°, 15°, 0°, -5°, and 0° sequentially (Figure 1). Each probe contained one source and one detector fiber for NIRS, and one source and two detector fibers for DCS measurements. The source-detector separation was 2.5 cm for both techniques. All fibers were custom made with tips bent at 90°.

2.2. Optical Method: Background And Analysis

Near-infrared photons undergo thousands of scattering events before reaching a detector displaced 3 cm from the source fiber at the tissue surface (Figure 1). Photon absorption also occurs, mainly due to tissue oxy- and deoxy-hemoglobin, water and lipid. Scattering is dominated by cell organelles, and a detectable amount of scattering comes from red blood cells (RBCs). If photons are scattered from moving RBCs, then the diffuse light intensity on the tissue surface will fluctuate in time. The resultant fluctuations of the detected intensity are measured by DCS. NIRS measures the differential change in the transmitted light intensity at multiple wavelengths due to absorption and scattering which, in turn, depend on changes in concentrations of oxy- and deoxy-hemoglobin (ΔHbO$_2$ and ΔHb) among other factors.

The "detection volume" depends on the tissue optical properties and the source-detector separation (Figure 1). Tissue optical properties or tissue dynamics within this
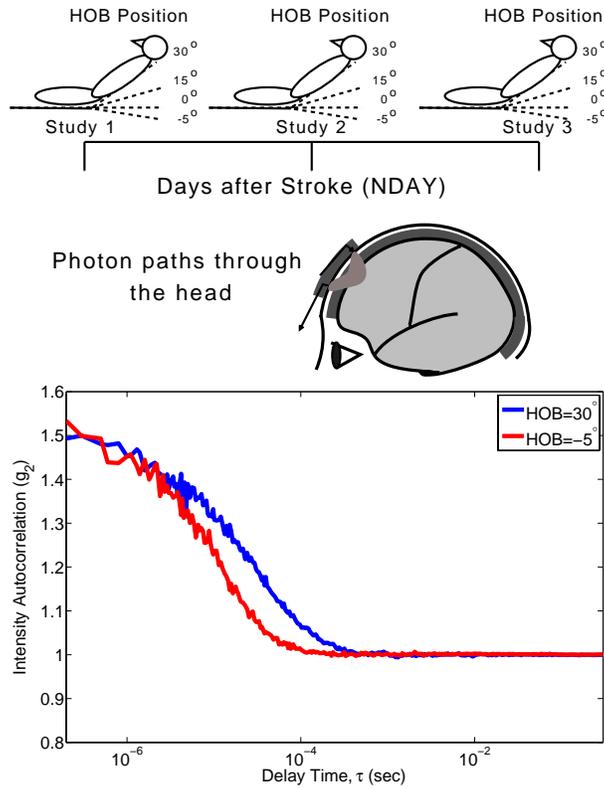
Fig. 1. Illustration of the measurement protocol (top), the probe positioning (middle), and the corresponding volume interrogated by the diffusing photons . (Bottom) Sample intensity auto-correlation data measured at HOB = 30° and -5°.

volume, such as those due to CBF variation from HOB positional changes, are detectable in the decay rate of the DCS intensity auto-correlation function ($g_2(\tau)$) (see Figure 1 for example data) or in the amplitude and phase of the diffusing wave NIRS signal. The DCS analysis employed a semi-infinite, homogeneous medium model for the head [31, 32, 35, 36, 49]. This model was iteratively fit to the measured auto-correlation functions and a flow-index for each hemisphere was extracted in seven second intervals. For NIRS, a modified Beer-Lambert equation [62, 63] with assumed photon path-lengths from the literature was used to analyze data [35, 36]. NIRS calculations report ΔHbO_2, ΔHb and their sum relative to the 30° baseline (i.e. $\Delta HbO_{2,30°}$, $\Delta Hb_{30°}$, $\Delta THC_{30°}$). DCS flow indices for each HOB angle were averaged and divided by the average flow index at the 30° baseline, providing CBF relative to that at 30°, i.e. $rCBF_{30°}$.

Here we present a simple outline of data analyses schemes that are described more fully in references [35, 36, 49].

2.2.1. Differential pathlength method for NIRS:

In order to estimate oxy- and deoxy-hemoglobin concentration changes in a rapid and simple manner we employed the so-called "differential pathlength method" [64–66]. This formulation can be derived approximately from the diffusion equation approach using Green's function solutions (in our case, in the semi-infinite, homogeneous geometry) [67].

In this formulation, the standard Beer-Lambert law is modified to account for the lengthening of the mean photon pathlength due to scattering and absorption effects in tissue. A "differential pathlength factor" (DPF) is introduced, which is the ratio of the mean photon pathlength to the physical separation of the source-detector pair. The DPF depends on experimental conditions such as geometry and wavelength and has minimal dependence on source-detector separation for large ($\sim$2 cm) separations [66]. Let $I(t,\lambda)$ be the light intensity measured by the source-detector pair at time, t, and employing light with wavelength (λ). Furthermore, let $I_0(<t_{30°}>,\lambda)$ be the average intensity measured by the same source-detector pair and wavelength on the same subject with the HOB at 30°. The differential pathlength approach relates changes in attenuation, $\Delta A(t,\lambda) = \ln \frac{I(t,\lambda)}{I_0(<t_{30°}>,\lambda)}$, to the change in tissue absorption ($\Delta\mu_a(t,\lambda)$) between measurement states, i.e.

$$\Delta A(t,\lambda) = \ln \frac{I(t,\lambda)}{I_0(<t_{30°}>,\lambda)} = -\Delta\mu_a(t,\lambda)DPF(\lambda)r \ . \tag{1}$$

Here r is the source-detector separation and the subscript "0" is used to denote the baseline measurement. $\Delta Hb_{30°}$ and $\Delta HbO_{2,30°}$ concentration changes can be calculated from $\Delta\mu_a(\lambda)$ at several wavelengths, using values from the literature for the extinction coefficients of $(\epsilon_{Hb}(\lambda),\epsilon_{HbO_2}(\lambda))$ [68] and the DPF values for an average, healthy adult head (DPF(λ_{690})=6.5, DPF(λ_{785})=6.4, DPF(λ_{830})=5.8) [64, 65] . Hemoglobin concentration changes are calculated by solving the following matrix equation at each time point;

$$\begin{bmatrix} \Delta\mu_a(\lambda_1,t) \\ \Delta\mu_a(\lambda_2,t) \end{bmatrix} = \begin{bmatrix} \epsilon_{Hb}(\lambda_1,t) & \epsilon_{HbO_2}(\lambda_1,t) \\ \epsilon_{Hb}(\lambda_2,t) & \epsilon_{HbO_2}(\lambda_2,t) \end{bmatrix} \begin{bmatrix} \Delta Hb(t) \\ \Delta HbO_2(t) \end{bmatrix} \ . \tag{2}$$

In our case, we use all three wavelengths to improve the signal-to-noise ratio and reduce the effect of fluctuations due to erratic fluctuations of a single laser. A substantial literature exists on the weaknesses and strengths of this formulation [66, 69–72], and experimental tabulations of the differential pathlength factor, DPF, are available for several organs [64, 65]. It is beyond the scope of this paper to discuss more of the details of this commonly employed formulation. The resultant $\Delta\mu_a(t,\lambda)$ at 785nm is used in DCS analysis to include the (minimal) effects of changes in absorption over time on the correlation function measurements.

2.2.2. Semi-infinite approximation for DCS:

In most flow experiments the fundamental quantity of interest is the electric field ($E(\mathbf{r},t)$) temporal autocorrelation function $G_1(\mathbf{r},t,\tau) = \langle \mathbf{E}(\mathbf{r},t) \ \mathbf{E^*}(\mathbf{r}, t + \tau) \rangle$ or its Fourier Transform. Here the angle brackets $\langle \ \ \rangle$ denote ensemble averages or averages over time for actual measurements. τ is called the correlation or delay time. In this study, the solutions for the photon correlation diffusion equation in a semi-infinite geometry were employed [31, 32, 35, 36, 49]

$$G_1(r,t,\tau) = \frac{3\mu_s'}{4\pi} \left(\frac{e^{-K(t,\tau)r}}{r} - \frac{e^{-K(t,\tau)r_2}}{r_2} \right) \ , \tag{3}$$

where r is the source-detector separation and $r_2 = \sqrt{r^2 + (z_o + 2z_b)^2}$ is the separation between an "image source" and the detector, $z_o = \frac{1}{\mu_s'}$ is equal to the random walk step, $z_b = \frac{2}{3\mu_s'}\frac{1+R_{eff}}{1-R_{eff}}$ is the distance of an imaginary boundary, R_{eff} is the reflection coefficient which depends on the ratio of the indices of refraction of tissue and air,

$K^2(t,\tau) = (\mu_a(t,\lambda_{785}) + \frac{1}{3}\alpha\mu'_s k_0^2 < \Delta r^2(t,\tau) >)/(3\mu'_s)$, μ'_s is the tissue reduced scattering coefficient (assumed to be constant over time), k_o is the wavevector of the photons in the tissue, $\langle \Delta \mathbf{r_s}^2(t,\tau) \rangle$ is the mean-square displacement in time τ of the scattering particles (i.e. red blood cells), and α represents the fraction of photon scattering events in tissue from moving cells.

Experimentally, we measure the intensity $(I(t))$ autocorrelation function, $g_2(r,t,\tau) = < I(t)I(t+\tau) > / < I(t) >^2$ which is related to the normalized field correlation function, $g_1(r,t,\tau) = G_1(r,t,\tau)/ < E(t)E^*(t) >$, by the Siegert relation;

$$g_2(r,t,\tau) = 1 + \beta|g_1(r,t,\tau)|^2 \ . \tag{4}$$

β is a parameter that depends on the source coherence, detection optics, ambient light and other external factors. In our experiments, β is allowed to be time dependent and is fitted and calculated from the measured data. While we see small variations in β of less than 0.1, accounting for them reduces signal fluctuations (unpublished phantom data).

The correlation diffusion equation can have different forms depending on the nature of the particle motion, and on the variations of these motions with position in the sample. We use a formulation wherein the mean-square displacement $\langle \Delta \mathbf{r_s}^2(t,\tau) \rangle = 6D_B(t)\tau$, red blood cells are taken to undergo an "effective" Brownian motion with a diffusion coefficient D_B. Note D_B is not the particle diffusion coefficient due to standard Brownian motion described by Einstein [73]. We then fit the measured autocorrelation function using Equation 3 for a "blood flow index" (i.e. $BFI(t) = \alpha D_B(t)$). As discussed in Section 1, we have previously shown that changes in a fitted $BFI(t)$ measure changes in CBF relatively accurately.

2.3. Instrumentation

A portable custom-built instrument was employed [35, 49]. DCS uses a long coherence length laser (785 nm). Three lasers (690nm, 785nm, 830nm) modulated at 70 MHz were used for NIRS. For DCS, the output of four high sensitivity avalanche photo-diode detectors operating in photon-counting mode were fed to a correlator board which computed the intensity auto-correlation functions in real time. For NIRS, a homodyne detection scheme with two detector channels was used [35, 49].

The data acquisition was interleaved between NIRS and DCS. For each probe, first NIRS data was acquired for 0.5 seconds, then DCS data was acquired for 3 seconds. This gives a total of 7 seconds of measurement time per data point since there are two probes. The fitted results reflect the mid-point of the acquisition period with respect to the start of the study.

2.4. Statistical Analysis

Data for each parameter was stored as a continuous variable over time. The data was then averaged for the last four minutes of each HOB position to avoid potential transient effects. On a few occasions, the patient condition changed transiently (e.g. the patient spoke), and we have carefully marked and avoided those times in our averaging. This averaged data was used in the statistical analysis.

To estimate and test for changes in mean rCBF and hemoglobin concentrations, we fit a linear mixed effects (LME) model (library "nlme" in R, http://www.r-project.org) [74], accounting for correlations between repeated measurements for each patient. Tests of relevant coefficients from the model were two-sided and used a Type I error rate of 0.05. We assessed changes in mean rCBF and mean hemoglobin concentrations as

a function of three factors: HOB angle, the presence of an infarction in a given hemisphere, and the number of days since reported stroke onset (NDAY). The variability was modeled as a function of the side of infarction based on analysis of residuals and the Akaike Information Criteria [75]. Significance factors of interest were assessed using a likelihood ratio test for appropriate nester models.

To assess the measurement repeatability for individual patients, the correlation coefficient (R) between paired measurements at a HOB of 0° was calculated. Clinical data were described using mean±standard error.

Table 1. Detailed patient characteristics (see Section 2.1 for details).

	Age (years)	Gender	Race	Risk Factors	Study Days
	General Characteristics				
1	70	F	C	STR,TOB	3,7
2	53	M	AA	STR,HTN,LIP,TOB	1,2,4
3	57	M	C	TOB	2
4	83	M	C	CAD,CHF,DM,AFIB	2,3,5
5	87	F	AA	HTN,AFIB,TOB	3,4
6	75	F	AA	STR,HTN,CHF,AFIB	2,3,4
7	59	M	AA	TOB	2,3
8	47	F	C	TOB	3,4
9	73	F	C	HTN	3,4,5
10	58	M	AA	HTN,TOB	1,4,7
11	44	F	AA	None	2,3,5
12	56	F	AA	HTN,TOB	1,2,3
13	93	F	AA	HTN,LIP	2,5
14	75	M	AA	HTN,LIP	2,3,4
15	47	F	C	TOB	2,3,6
16	47	F	C	STR,TIA,HTN,DM,LIP	4,7,11
17	79	M	C	HTN,LIP,CAD,CHF,TOB	2

|	Stroke Lat.	Vessel Inv.	Brain Reg. Inv.	NIHSS	Etiology	Orth. Symp.
	Stroke Related					
1	Right	MCA	F,T	18	CE	No
2	Right	MCA	F,T	9	CE	No
3	Left	ACA,MCA	F,P	2	LAS	No
4	Right	MCA	F,T,P	18	CE	No
5	Left	MCA	F,T,P	24	CE	No
6	Left	MCA	F,T,P	22	CE	No
7	Left	ICA	F,P	6	LAS	Yes
8	Right	MCA	F	5	CE	No
9	Left	MCA	F,T,P	20	CRYP	No
10	Left	MCA	F,T	3	LAS	No
11	Right	MCA	F,T,P	18	OTHER	No
12	Left	MCA	F,T,P	15	CRYP	No
13	Left	MCA	F,T,P	26	OTHER	No
14	Left	MCA	F,T,P	24	CRYP	No
15	Left	MCA,ACA	F,T,P	19	CE	Yes
16	Left	MCA	F,T	7	SAO	Yes
17	Left	MCA	F,T,P	22	CRYP	No
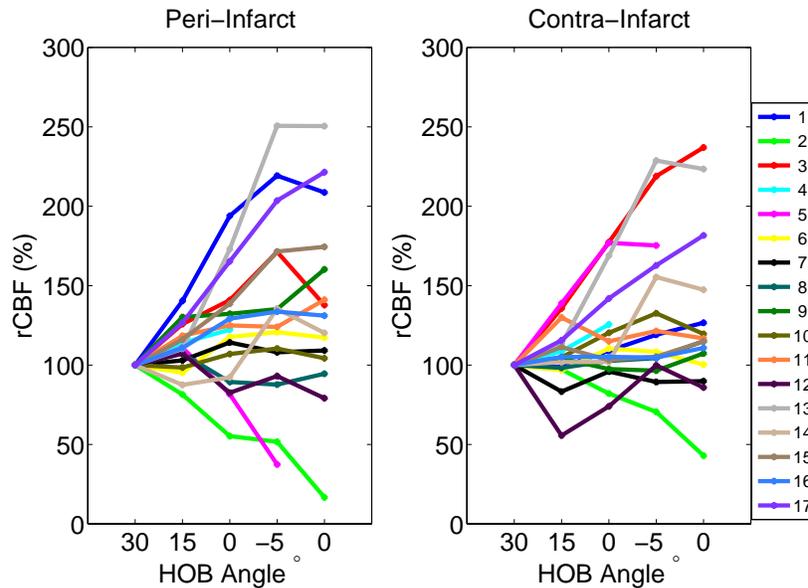
Fig. 2. Variation in CBF due to HOB positioning on first study day from peri- and contra-infarct hemispheres are shown for all patients (different color per patient)

3. Results

Reliable measurements were obtained from all subjects. Figure 1 shows typical measured temporal auto-correlation functions with a faster decay rate when the HOB is lowered from 30° to -5°, indicating an increase in CBF.

The seventeen AIS patients aged between 44 and 93 years (65±16), with admission NIHSS score from 2 to 26 (15±8). The mean number of days since reported stroke onset (NDAY) for the first optical study was 2.2±0.8 days. The middle cerebral artery (MCA) territory only was involved in 14 cases while the anterior cerebral artery territory was also involved in 3 additional cases. Orthostatic symptoms were present in three patients. Patient details are summarized in Table 1 and statistical findings from the optical data in Table 2.

$rCBF_{30°}$ in the AIS group showed a large variability between subjects, presumably due to differences in their clinical condition. Figure 2 shows variations in CBF with positioning on the first study day for all patients. Results from subsequent days had similar levels of variability (data not shown).

Repeated measurements at flat HOB, i.e. when lowering from 15° and when raising from -5°, showed a strong correlation to initial value (R=0.96), indicating excellent repeatability within each study day (R=0.96). HOB positioning was significantly associated with changes in frontal hemispheric $rCBF_{30°}$ in both infarct (p=0.008) and non-infarct (p=0.005) hemispheres. The presence of an "infarct" in a given hemisphere was significantly associated with increased variability in $rCBF_{30°}$ versus HOB position (p=0.02). Figure 3(a) shows one representative result on the third day after stroke onset from a 70 year old female with a right MCA occlusion. During rest periods between changes of HOB, the variations in measured $rCBF_{30°}$ were smaller than changes due to HOB angle, and a large discrepancy was observed between hemispheres.

Similarly, $\Delta HbO_{2,30°}$, $\Delta Hb_{30°}$ and $\Delta THC_{30°}$ in the AIS group showed a large vari-

Table 2. Statistical findings in acute ischemic stroke (AIS) group. SEM=Standard Error of Mean. Bold font implies statistical significance .

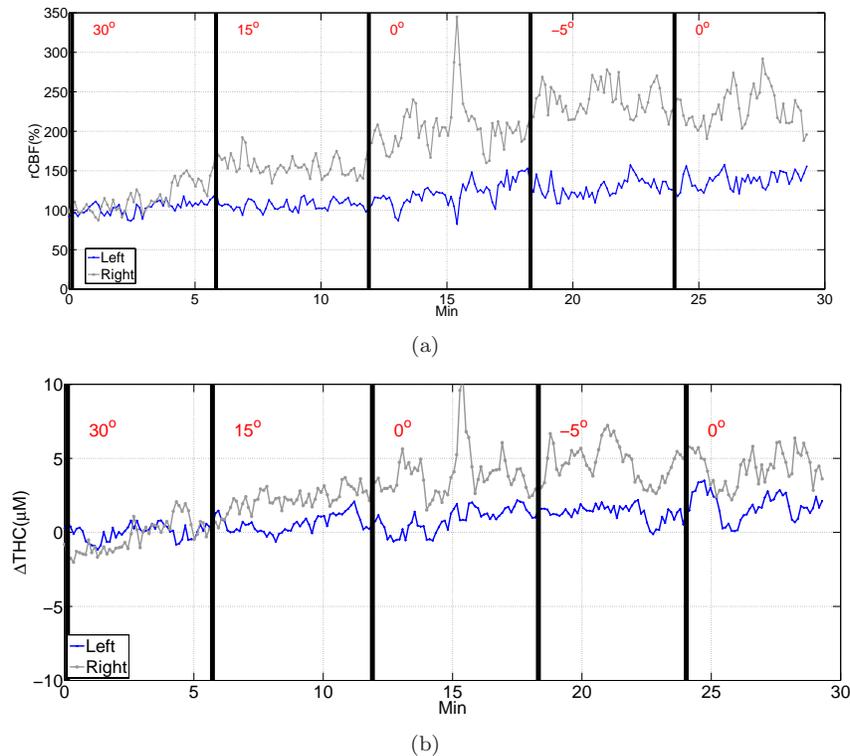|		CBF			
		Infarct		Non-Infarct	
		$rCBF_{30°}$ (SEM) (%)	p-value	$rCBF_{30°}$ (SEM) (%)	p-value
HOB	15°	112(9)		105(8)	
	0°	130(7)	**0.008**	125(7)	**0.005**
	-5°	137(8)		127(8)	
NDAY	≤ 2	124(9)		125(8)	
	3-4	133(8)	0.3	123(8)	0.1
	>4	121(9)		110(9)	
		Infarct Effect:	p-value		
		YES	**0.02**		
		Oxy-Hemoglobin			
		Infarct		Non-Infarct	
		ΔHbO_2(SEM) (μM)	p-value	ΔHbO_2(SEM) (μM)	p-value
HOB	15°	1.6(1.2)		0.7(1.4)	
	0°	4.2(1.0)	**0.004**	2(1)	0.15
	-5°	5.5(1.2)		3(1.2)	
NDAY	≤ 2	4.2(1.2)		2.8(1.4)	
	3-4	2.9(1.2)	0.5	1.3(1.1)	0.3
	>4	4.4(1.3)		0.8(1.3)	
		Infarct Effect:	p-value		
		YES	$\mathbf{4x10^{-5}}$		
		Deoxy-Hemoglobin			
		Infarct		Non-Infarct	
		ΔHb(SEM) (μM)	p-value	ΔHb(SEM) (μM)	p-value
HOB	15°	0.3(0.5)		-0.3(0.5)	
	0°	0.4(0.5)	0.6	-0.5(0.6)	0.9
	-5°	0.9(0.6)		-0.3(0.7)	
NDAY	≤ 2	-0.1(0.4)		0.1(0.5)	
	3-4	1(0.5)	0.1	-1.1(0.6)	0.1
	>4	1.3(0.6)		-0.05(0.7)	
		Infarct Effect:	p-value		
		YES	**0.001**		
		Total Hemoglobin			
		Infarct		Non-Infarct	
		ΔTHC(SEM) (μM)	p-value	ΔTHC(SEM) (μM)	p-value
HOB	15°	1.8(1.5)		0.3(1.7)	
	0°	4.5(1.4)	**0.03**	1.5(1.5)	0.4
	-5°	6.3(1.7)		2.6(1.8)	
NDAY	≤ 2	4.1(1.4)		2.9(1.6)	
	3-4	3.6(1.6)	0.7	0.4(1.6)	0.3
	>4	5.3(1.8)		0.5(1.9)	
		Infarct Effect:	p-value		
		YES	$\mathbf{4x10^{-5}}$		

Fig. 3. (a) rCBF$_{30°}$ and (b) ΔTHC$_{30°}$ as a function of time with HOB angle from a patient with right MCA occlusion. HOB position is a significant factor in both hemispheres, but a larger effect is observed in the infarct (right) hemisphere. Blue(gray) indicate left(right) hemispheres.

ability between subjects but with excellent repeatability (R=0.94). Unlike rCBF$_{30°}$, the HOB effect on ΔHbO$_{2,30°}$ and ΔTHC$_{30°}$ was significant only in the infarct (p=0.004 and p=0.03) but not in the non-infarct (p=0.15 and p=0.4) hemisphere. ΔHb$_{30°}$ was not significant in either hemisphere (p=0.6 and p=0.9). Nevertheless, the presence of an "infarct" in a given hemisphere was significantly associated with increased variability for all quantities. These findings are in qualitative agreement with rCBF$_{30°}$ findings. NIRS data is, however, harder to interpret since local changes in oxy- and deoxy-hemoglobin concentration are dependent on complex parameters such as the local oxygen extraction fraction. Figure 3(b) shows ΔTHC$_{30°}$ from the same patient. During rest periods between changes of HOB, the variations in measured ΔTHC$_{30°}$ are smaller than changes due to HOB angle and a very large discrepancy is observed between the infarct and non-infarct hemispheres.

Several measurements were conducted in each patient between 1 and 11 days post-stroke. To consider the effect of NDAY, we categorized each measurement as occurring between 1-2, 3-4, or >4 days after the reported stroke onset. We anticipated that NDAY might have a larger effect on the infarct hemisphere than on the non-infarct hemisphere, but this was not observed. Bi-variate analysis (including NDAY with HOB) did not change our conclusions.

We note that approximately 75% of the patients had maximal CBF and THC at 0°

or -5°. However, four ($\sim$25%) patients exhibited maximal CBF and THC at HOB>0° which we denote as being "paradoxical".

Eight subjects were enrolled in the control VRF group (mean age 64 years). Both hemispheres showed similar $rCBF_{30°}$ response to changes in HOB angle. At a given angle, the variations in $rCBF_{30°}$ due to physiology and instrumental noise were smaller than changes due to HOB angle (Figure 4(a)). The $\Delta THC_{30°}$ results agree qualitatively with $rCBF_{30°}$ (Figure 4(b)). As expected, there is no statistical difference between two hemispheres (p=0.57) with $rCBF_{30°}$ depending equally strongly on HOB angle (p=0.0001). Repeated measurements at flat HOB, i.e. when lowering from 15° and when raising from -5°, showed a strong correlation to initial value (R=0.95), confirming measurement reproducibility. Similar results where obtained with THC but without achieving significance with HOB changes.

Finally, in an analysis comparing randomly selected hemispheres for all subjects in the VRF group to the infarcted hemispheres for all subjects in the AIS group, a statistically significant difference was observed between the two groups for $rCBF_{30°}$ (p=0.02) and for $\Delta THC_{30°}$ (p=0.0001).

(a)

(b)
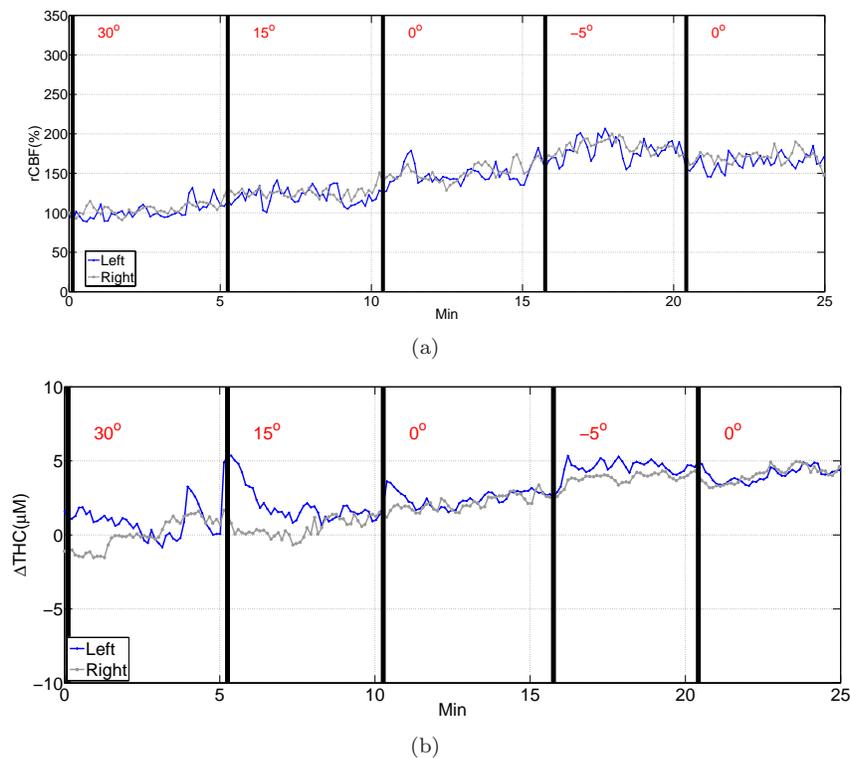
Fig. 4. $rCBF_{30°}$ (a) and $\Delta THC_{30°}$ (b) changes over time with HOB angle in a subject with vascular risk factors. Blue(gray) lines indicate left(right) hemispheres. Thick vertical bars indicate HOB changes to the labeled angle.

4. Discussion

This study demonstrates the feasibility of hybrid DCS-NIRS technology for monitoring differences in autoregulatory impairment between the affected and unaffected hemi-

spheres in acute stroke patients. As predicted, the presence of an ischemic infarct was significantly associated with changes in ipsilateral $rCBF_{30°}$ as HOB positions varied. In addition, repeat measurements at 0° HOB showed a high degree of intra-subject repeatability (R>0.9), suggesting that DCS provides reproducible measurements of CBF. These findings provide the first demonstration of DCS as an effective modality for measuring changes of CBF in acute stroke patients, building upon prior studies that used DCS to measure CBF in healthy human subjects [35, 36].

A key observation was the variable impact of acute ischemic stroke on cerebrovascular autoregulation. While the results for the VRF (control) group were similar between individuals and did not show any significant variations in $rCBF_{30°}$ response between hemispheres, the AIS group showed a large variability between subjects. Most importantly, for the AIS group a statistically significant difference was observed between infarct and non-infarct hemispheres. For the AIS group, the majority of patients displayed maximal CBF at a HOB angle of 0° to -5°, while approximately 25% exhibited maximal CBF at an elevated HOB angle of 15° to 30°. All subjects of the VRF group, however, showed maximal CBF at -5°. The basis for a paradoxical response is uncertain, but could be due to elevated intracranial pressure (ICP), hemodynamic consequences of heart failure, or autonomic dysfunction. Similar paradoxical responses have been previously reported in traumatic brain injury [76]. Close examination of a recent work that used NIRS to monitor blood oxygen saturation during postural changes in acute stroke patients reveal a paradoxical response and large intra-subject variability in line with our results [30].

Although measurements of ICP and cerebral perfusion pressure (CPP) were not available in our patients, and the precise mechanism for the paradoxical responses could not be determined, these findings suggest that flat HOB may not represent the optimum therapy for all patients with acute hemispheric stroke. We note that DCS results were recently compared to changes in ICP and CPP during HOB changes in traumatic brain injury patients indicating a close correlation between hemodynamic parameters measured by DCS-NIRS and perfusion pressures (ICP and CPP) in instances of damagedautoregulation [45, 51, 54]. Furthermore, paradoxical responses similar to those observed in the AIS group reported here were confirmed in this patient group [45, 51, 54].

Some patients did not exhibit a change in CBF with different HOB angles, suggesting that cerebrovascular autoregulation is not universally disrupted. In patients with normal autoregulation, the risks of flat positioning might be avoided altogether if a diagnostic modality such as DCS were available to determine whether CBF was dependent on positioning. Pneumonia occurs in approximately 5% of acute stroke patients, with aspiration pneumonia accounting for 60% of the cases [77]. There is a strong link between aspiration risk and a flat HOB [78], especially in stroke patients with decreased consciousness. Other common complications associated with a flat HOB position and immobilization are symptomatic deep venous thrombosis [79], and pulmonary embolism, which causes up to 25% of early deaths after stroke [80].

Another finding was that NDAY was not significantly associated with HOB-related CBF changes across the population (p=0.11). The unpredictable response of CBF to HOB angle over time suggests that cerebrovascular autoregulation recovers at a variable rate from patient to patient. Some previous studies have suggested the degree of autoregulatory impairment may be related to the malignancy and worsening of the stroke, [81] providing a further rationale for the development of real-time monitoring of CBF at the bedside.

Our finding that flat HOB position improves CBF with a stronger change in the

infarcted hemisphere in *most* ($\sim$75%) of AIS subjects is generally consistent with previous reports on impairment of autoregulation in acute stroke patients [16, 30, 82, 83]. Schwarz *et al* [16] found that CPP was maximal at 0° corresponding to elevated mean arterial pressure (MAP) and ICP. Similarly, mean blood flow velocity ing the middle cerebral artery (V_mMCA) measured by TCD was also maximal at 0°. They did not observe any subjects who showed a paradoxical response. Furthermore, in nearly half of their patients V_mMCA could not be measured on the infarcted hemisphere since there was a permanent occlusion of the MCA. Where V_mMCA was measured bilaterally, there was a larger effect on the infarcted hemisphere consistent with our findings. A newer study by Wojner-Alexander *et al* [82] also observed that V_mMCA was maximal at 0° HOB.

HOB-related CBF changes observed in the VRF group are generally consistent with prior studies of positional blood flow in patients with ischemic risk factors performed using TCD. Lipsitz et al. [84] found that mean MCA blood flow velocity decreased by 14% on continuous TCD monitoring of elderly hypertensive subjects during change from the sitting to standing position. Asil et al. [85] similarly demonstrated a 13-16% decrease in MCA blood flow velocity in diabetic patients 1.5 minutes after changing from a supine to upright position. Changes in microvascular CBF observed in the present study were somewhat larger, which may be attributable to differences in the specific vasculature probed by TCD and DCS and to differences in the positioning protocol used. Future studies with concurrent DCS and TCD will be required to better characterize the relationship between these measures.

Several future methodological improvements can be anticipated based on corrections to the technical limitations of this study. We have previously shown that DCS does indeed penetrate to the cortex and measures local CBF [35, 36]. Nevertheless, all such diffuse optical methiologies hold potential for signal contamination from changes of blood flow in superficial layers such as the scalp. We note, however, that by self-normalizing data from each hemisphere to data taken at 30° elevation, we effectively ameliorate the effects of such systemic changes. Presumably, the only observable hemispheric changes to survive normalization are due to hemodynamic differences in the cortical tissue. Future studies may incorporate both small and large source-detector separations to allow separation of scalp and cortex contributions. In addition, quantification with the diffuse optical method can be improved by knowledge of skull thickness derived by CT or MRI.

In the present studies, optical probes were placed on the forehead. Accordingly, we limited our investigation to acute stroke patients whose infarct or ischemic penumbra involved the frontal lobe cortex. A follow-up study is currently underway to assess the feasibility of monitoring CBF changes in other regions. If successful, future instruments with larger probe arrays could be used to monitor CBF throughout the cortex.

While the primary aim of this study was to explore the sensitivity of DCS for detecting hemodynamic effects of HOB changes in patients with acute ischemic stroke, we also obtained concurrent NIRS data for comparison. NIRS measurements of THC and HbO_2 most closely approximate CBF, and showed reasonable agreement with DCS measurements in the ischemic hemisphere. Indeed, all NIRS parameters showed more significant associations with the infarcted hemisphere than CBF by DCS, whereas only CBF showed significant HOB effects in the unaffected hemisphere and in the control group with vascular risk factors. The sensitivity of NIRS to ischemic physiology probably reflects its sensitivity to both CBF and metabolism, and the differential sensitivities of DCS and NIRS suggest that they will likely provide complementary information in

the management of acute ischemic stroke and other central-nervous system disorders.

Although these data are preliminary, the observed variability in autoregulatory impairment and recovery has implications for individualized therapy in stroke management. Current guidelines from the American Stroke Association state that patients with acute, ischemic stroke should be empirically placed in a flat HOB position upon admission to the hospital. There is no formal recommendation on how long to keep a patient supine, but the authors recommend that stroke patients be observed closely during the transition to sitting and standing for any new neurological symptoms [86]. Our data suggest that this empirical approach to HOB manipulations in acute stroke patients may not be optimal for some subjects, and suggests the possibility that in the future, individualized management based on CBF monitoring could improve stroke outcomes by minimizing the risk-to-benefit ratio of hemodynamic interventions such HOB positioning, volume expansion, and hypertensive therapy. Bedside monitoring of stroke patients with DCS and NIRS may also allow changes in CBF and metabolism to be detected prior to the onset of clinical symptoms.